EBioMedicine 49 (2019) 72–81

Contents lists available at ScienceDirect

EBioMedicine

journal homepage: www.elsevier.com/locate/ebiom

Research paper

Potentiation of Kras peptide cancer vaccine by avasimibe, a cholesterol modulator

Jing Pan[a,1], Qi Zhang[a,1], Katie Palen[b], Li Wang[c], Lifen Qiao[a], Bryon Johnson[b], Shizuko Sei[d], Robert H. Shoemaker[d], Ronald A. Lubet[d], Yian Wang[a], Ming You[a,*]

[a] Center for Disease Prevention Research and Department of Pharmacology & Toxicology, Medical College of Wisconsin, Milwaukee, WI, USA
[b] Department of Medicine, Medical College of Wisconsin, Milwaukee, WI, USA
[c] Department of Translational Hematology and Oncology Research, Cleveland Clinic Foundation, Cleveland, OH, USA
[d] Chemopreventive Agent Development Research Group, Division of Cancer Prevention, National Cancer Institute, Bethesda, MD, USA

ARTICLE INFO

Article history:
Received 12 March 2019
Revised 22 October 2019
Accepted 23 October 2019
Available online 31 October 2019

Keywords:
Chemoimmunoprevention
Kras
Peptide vaccine
Avasimibe
Cholesterol metabolism
T cell

ABSTRACT

Background: No effective approaches to target mutant Kras have yet been developed. Immunoprevention using KRAS-specific antigenic peptides to trigger T cells capable of targeting tumor cells relies heavily on lipid metabolism. To facilitate better TCR/peptide/MHC interactions that result in better cancer preventive efficacy, we combined KVax with avasimibe, a specific ACAT1 inhibitor, tested their anti-cancer efficacy in mouse lung cancer models, where Kras mutation was induced before vaccination.

Methods: Control of tumor growth utilizing a multi-peptide Kras vaccine was tested in combination with avasimibe in a syngeneic lung cancer mouse model and a genetically engineered mouse model (GEMM). Activation of immune responses after administration of Kras vaccine and avasimibe was also assessed by flow cytometry, ELISpot and IHC.

Findings: We found that Kras vaccine combined with avasimibe significantly decreased the presence of regulatory T cells in the tumor microenvironment and facilitated CD8+ *T* cell infiltration in tumor sites. Avasimibe also enhanced the efficacy of Kras vaccines target mutant Kras. Whereas the Kras vaccine significantly increased antigen-specific intracellular IFN-γ and granzyme B levels in CD8+ *T* cells, avasimibe significantly increased the number of tumor-infiltrating CD8+ *T* cells. Additionally, modulation of cholesterol metabolism was found to specifically impact in T cells, and not in cancer cells.

Interpretation: Avasimibe complements the efficacy of a multi-peptide Kras vaccine in controlling lung cancer development and growth. This treatment regimen represents a novel immunoprevention approach to prevent lung cancer.

1. Research in context

1.1. Evidence before this study

Kras mutations are responsible for driving progression of multiple types of human cancers, including lung cancer. However, efforts to target Kras-driven cancers preventively or therapeutically have, to date, been unsuccessful. Cancer vaccines have the potential to activate adaptive immune responses to eliminate cells harboring mutant Kras. We recently developed a multi-peptide Kras vaccine (KVax) that demonstrates anti-tumor efficacy in lung tumors prior to the expression of mutant Kras. Avasimibe, an Acyl-coenzyme A: cholesterol acyltransferase 1 (ACAT1) inhibitor that modulates cholesterol metabolism, was recently discovered to enhance the effector function of tumor-specific CD8+ cytotoxic T cells.

1.2. Added value of this study

We found that avasimibe significantly decreased the number of regulatory T cells in the tumor microenvironment and increased the presence of effector CD8+ *T* cells. Avasimibe also enhanced the efficacy of Kras vaccine in controlling development and growth of Kras lung cancer. The biochemical effects of avasimibe on modulation of cholesterol synthesis in these models were limited to T cells, and not cancer cells.

* Corresponding author.
E-mail address: myou@mcw.edu (M. You).
[1] These authors contributed equally.

https://doi.org/10.1016/j.ebiom.2019.10.044

1.3. Implications of all the available evidence

The studies described herein identify a potential approach to prevent Kras-driven lung tumorigenesis in high-risk populations by combining a multi-peptide Kras vaccine with avasimibe, a cholesterol-modulating agent that alters cholesterol levels in T cells. This is a novel immune approach to prevent Kras-driven cancers.

Lung cancer is the leading cause of cancer death worldwide for both men and women. Mutations in Kras, a major driver of lung cancer, are present in approximately 30% of lung cancer patients [1,2]. Kras mutations are also the major driver for several other cancers including those originating from pancreas and colon, but efforts to target Kras-driven cancers preventively or therapeutically have been unsuccessful [1-3]. The RAS family of proteins have proven difficult to target due to the complexity of their signal transduction, the presence of feedback loops, redundancy between isoforms, heterogeneous expression within tumors, and rapid resistance from mutations in downstream proteins such as RAF and MEK [3]. Since therapeutic efforts to inhibit RAS using small molecule inhibitors have been ineffective, peptide vaccination against tumor-specific mutant forms of RAS has begun to garner significant attention [4-6]. Development of this strategy is particularly important for high-risk individuals such as former or current smokers, and those with resected primary lung cancer who are at high risk for relapse.

Cancer prevention vaccines are under development for high-risk individuals with or without premalignant lesions to activate adaptive immune responses against mutant proteins that drive oncogenesis, such as Kras [5,6]. Past strategies to target mutant Kras have primarily utilized vaccines containing short peptides. While these approaches have demonstrated safety and immunogenicity, they have not demonstrated efficacy in controlling tumor development or growth [7]. We recently developed a multi-peptide Kras vaccine (KVax) that contains several long, as opposed to short, peptides [15–20 amino acids (AA)], with high-affinity binding to multiple MHC class II alleles [4]. The mutant vaccines target both wild-type and G12D mutant Kras that are conserved between humans and mice. When vaccination with this Kras multi-peptide vaccine was initiated prior to expression of mutant Kras in an inducible CCSP-Kras murine lung cancer model, striking anti-tumor efficacy was observed [4]. However, high-risk individuals may already express mutant Kras prior to or concurrent with the onset of lung tumorigenesis, and constitutively active Kras may play a role in actively subverting anti-tumor immune responses, thereby hampering the efficacy of KVax. Therefore, testing the efficacy of the multi-peptide KVax after development of Kras-driven lung cancer model is of clinical importance.

Immunoprevention using tumor-specific antigenic peptides to activate tumor-specific T cells is dependent on T cell receptor (TCR)/peptide/MHC interactions [8,9]. TCR signal transduction is influenced by lipid metabolism, in part because non-esterified cholesterol is a major component of lipid rafts which localize TCR to sites of antigen presentation [10,11]. Acyl-coenzyme A:cholesterol acyltransferase 1 (ACAT1) is the dominant enzyme in CD8+ *T* cells that converts free cholesterol to cholesteryl esters and attenuates lipid raft formation [12]. ACAT1 deficiency leads to higher plasma membrane cholesterol levels in CD8+ *T* cells, and this correlates with higher TCR signaling levels after stimulation [13]. Avasimibe, a specific ACAT1 inhibitor is a potent cholesterol lowering compound that is currently being developed as a treatment for hyperlipidemic-induced atherosclerosis and Alzheimer's disease and has demonstrated safety in preclinical models and in human clinical trials for these diseases [14,15]. Recently, avasimibe has also been found to promote anti-tumor immune responses by increasing the effector function of tumor-specific CD8+ cytotoxic T cells [13].

To ameliorate mutant Kras-mediated immune suppressive tumor-mediated effects and more generally, enhance the efficacy of KVax, we combined KVax with avasimibe. We first evaluated immunopotentiation mediated by avasimibe in Kras-driven lung tumorigenesis and determined the tumor-intrinsic versus immune-mediated impact of ACAT1 inhibition. Second, we determined the efficacy of avasimibe in combination with KVax to prevent mouse lung tumorigenesis. Since CD4+ *T* cells are relatively resistant to avasimibe-mediated inhibition due to high expression of a second ACAT isoform ACAT2, and because KVax primarily induces MHC-II-restricted CD4+ *T* cell responses [4], we hypothesized that a combination of KVax (which drives the CD4+ *T* helper cell response) and avasimibe (which promotes the CD8+ *T* cell response) would provide an additive or synergistic benefit on improving the anti-tumor adaptive immune response. In support of our hypothesis, we found that the combination of avasimibe and KVax confers enhanced antitumor effects in a Kras-driven preclinical lung cancer model, supporting a role for this approach in preventing Kras-driven lung cancer in high-risk patients.

2. Materials and methods

2.1. Mouse models and treatments

LKR13 cells and $Kras^{LA1}$ mice, which express mutant $Kras^{G12D}$ on the sv129 background, were a generous gift from Dr. Jonathan M. Kurie (MD Anderson) [16,17]. Wild-type sv129 mice were purchased from the Jackson Laboratory. Mice were kept in the Biomedical Resource Center at the Medical College of Wisconsin, Milwaukee, WI, and all procedures were approved by the Institutional Animal Care and Use Committee (IACUC). LKR13 cells, originated from $Kras^{LA1}$ mice, were cultured in RPMI-1640 (Thermofisher, 11,875–093) supplemented with 10% FBS and 1% penicillin/streptomycin (complete RPMI1640). For syngeneic tumor graft experiments, LKR13 cells were trypsinized, washed with PBS filtered through a 30-μm strainer, and then 5×10^5 cells (in 0.1 ml of PBS) were inoculated subcutaneously into the right flanks of experimental and control mice. Tumor sizes were measured with a digital caliper. To analyze the functional effects of avasimibe on tumor-infiltrating T cells, LKR13 tumor-bearing mice with similar lung tumor size were divided into four groups. Starting on day 10 after tumor cell inoculation, 15 mg/kg.bw avasimibe (Selleck) was injected intraperitoneally into mice either 24 or 48 h before euthanization (short-term treatment), or every 2 days for longer-term treatment. For GEMM model experiments, 5–6 week old $Kras^{LA1}$ mice were divided into four groups: (a) control, in which mice received adjuvant and corn oil containing 0.5% DMSO, (b) KVax, in which mice were given adjuvant vaccine, (c) avasimibe, in which mice were given intragastric treatments of avasimibe dissolved in DMSO and diluted with corn oil (0.5% DMSO final) every 2 days, and (d) combined treatment, in which mice received both KVax and avasimibe.

2.2. Vaccine preparation and immunization

Kras peptide vaccine contains four peptides that represent different regions of Kras: Kras-G12D (KLVVVGADGVGKSALTI), Kras-61Wt (KLVVVGAGGVGKSALTI), Kras-63Wt (SALTIQLIQNHFVDE) and Kras-68Wt (FLCVFAINNTKSFED). The peptides were synthesized by Genemeds with >95% purity as assessed by HPLC. Mice were vaccinated with 50 μg of each peptide. Adjuvants used in the study included CpG (Invivogen), R848 (Invivogen) and anti-CD40 (Bioxell) (each delivered at 50 µg/mouse). The total vaccine volume was 100 μL/mouse. Mice were injected subcutaneously in the left flank

starting at 5 weeks of age, with booster vaccines given every two weeks for the first three boosts, and every 4 weeks thereafter as shown in Figs. 2a and 5a.

2.3. ELISPOT assay

Single cell suspensions were prepared by mechanically mash spleen through a 40 μm cell strainer (BD). Red blood cells were removed by ACK buffer, and cells were re-suspended in T media (RPMI1640, 10% FBS, 1% Penicillin/streptomycin, 1xβ-ME) after neutralization and wash. MAIPS4510 Multiscreen 96-well plate were coated with anti-interferon-γ capture antibody overnight at 4 °C, after wash and blocking with T media, 1.5–3.0 $\times$ 10^4 splenocytes were seeded into the MAIPS4510 plate, the cells were stimulated with peptides, concanavalin A (positive control), an HIV peptide (negative control), or medium only (negative control). When tumor cells were used for re-stimulation, 1.0 $\times$ 10^4 irradiated LKR13 tumor cells were co-cultured with splenocytes from vaccinated mice. After 72 h, the MAIPS4510 plates were washed and anti-interferon-γ detection antibody was added. After incubation at 4 °C overnight, wells were washed, and secondary antibody (BD) was added for 1∼2 hr. After a final wash with PBS, HRP-streptavidin was added. Following 1-hour incubation, the plates were kept at room temperature and AEC substrate was added for 5–25 min. The plates were then gently washed with cold tap water. After evaporation of fluid, an automated plate reader system (CTL Technologies) was used to image the plates and quantify spot numbers.

2.4. Lung tumor counting using H&E staining

Mouse lungs from $Kras^{LA1}$ mice were inflated, formalin fixed overnight and then stored in 70% ethanol. Surface tumor counting was conducted as previously described [18] using a dissecting microscope. Tumor volume for each tumor was calculated as $V = (4/3) \times \pi \times (L/2) \times (L/2) \times (D/2)$, in which tumor load was calculated as the sum of tumor volume from each animal [18] using a dissecting microscope.

Fixed lung tissues were further processed (Sakura Tissue Tek VIP5) for H&E or immunohistochemistry staining with anti-CD8 (Cell Signaling Technology, Inc.) or anti-pERK1/2 (Cell Signaling Technology, Inc.) antibodies. Three slides were selected per mouse for analysis, corresponding to ventral, midline and dorsal regions of the lung. IHC slides were scanned with the NanoZoomer HT slide scanner (Hamamatsu Photonics France SARL), the lung tumor area was evaluated using NanoZoomer Digital Pathology Virtual Slide Viewer software (Hamamatsu Photonic Co.). Positive cells were counted in three high-powered microscopic fields randomly chosen from each slide and expressed as a mean. The number of positive cells in the field was expressed as % of $CD8^+$ cells per mm^2 tumor area [19]. Data are shown as the mean ± SEM.

2.5. Flow cytometry

To analyze tumor-infiltrating T cells, tumors harvested from LKR13 syngraft tumors or $Kras^{LA1}$ primary tumors were minced into 1 mm^3 pieces and digested at 37 °C for 20 min with mouse tumor dissociation buffer (Miltenyi Biotec, CA) to generate single cell suspension per the manufacturer's instructions. Tumor-infiltrating leukocytes were enriched by using Ficoll-Paque (Stem cell, MA) gradient centrifugation.

Isolated cells were stained with fixable live/dead dye in PBS, washed, and then stained with BV786 anti-CD45, APC eFluro780 anti-CD3, FITC anti-CD4, BUV396 anti-CD8a, SB600 anti-CD19, PE-Cy7 anti-CD44, APC anti-CD62L, PE anti-CD25 antibodies and/or 7AAD. For intracellular cytokine staining, cells were stimulated for 2 h with PMA/Ionomycin/BFA, or 4 hours in complete RPMI medium containing Kras peptides, 10% FBS, 2 mM L-glutamine, 50 μM 2-mercaptoethanol, 1% penicillin-streptomycin, 1x monensin, 1x Brefeldin A (Thermofisher Sci). For Foxp3 staining, cells were then washed, fixed and permeabilized with Foxp3/Transcription Factor Staining Buffer set (Thermofisher) following manufacturer's instructions, and then stained with eFluor450 anti-Foxp3. For intracellular cytokine analysis, cells were fixed with 2% paraformaldehyde, permeabilized with 0.5% saponin, and stained with intracellular cytokine staining buffer containing Brefeldin A, APC anti-granzyme B, PE anti-IFN-γ and PE-Cy7 anti-TNF-α antibody, then analyzed by flow cytometry. T cells stained with isotype control antibody were used as negative controls. To detect myeloid derived suppressor cells (MDSC) in tumors, cells were stained with PerCP-Cy5.5 anti-CD45, FITC anti-CD11b, APC anti-CD11c, PE anti-Ly6G and PE-Cy7 anti-Ly6C Ab. Flow cytometry was conducted using an LSR Fortessa™ X-20 or LSR-II flow cytometer (Becton Dickinson). Data were analyzed using FlowJo software.

2.6. Cytokine analysis

Mouse Cytokine Array / Chemokine Array 31-Plex (MD31) were used for cytokine analysis (Eve's technologies); it analyzes a panel of 31 cytokines involved in T helper cell biology. The cytokines represented by this array are Eotaxin, G-CSF, GM-CSF, IFN-ɣ, IL-1α, IL-1β, IL-2, IL-3, IL-4, IL-5, IL-6, IL-7, IL-9, IL-10, IL-12 (p40), IL-12 (p70), IL-13, IL-15, IL-17A, IP-10, KC, LIF, LIX, MCP-1, M-CSF, MIG, MIP-1α, MIP-1β, MIP-2, RANTES, TNFα, and VEGF. Splenocytes from different groups of mice were stimulated with different peptides for 72 h, and then supernatant was collected and sent to EVE's Technologies for analysis.

2.7. Quantitative reverse transcription PCR

Total RNA was extracted from LKR13 tumor cells or CD8+ TILs isolated from tumors left untreated or treated with different doses of avasimibe using RNA Plus Micro kits (Qiagen). cDNA was synthesized with iScript kits (Qiagen), and quantitative reverse transcription PCR (qRT–PCR) conducted using Ssofast Evagreen (Qiagen) per the manufacturer's instructions. Primers used in qRT–PCR were as follows:

Nceh (forward, TTGAATACAGGCTAGTCCCACA; reverse, CAACGTAGGTAAACTGTTGTCCC);
Srebp1 (forward, GCAGCCACCATCTAGCCTG; reverse, CAGCAGTGAGTCTGCCTTGAT);
Srebp2 (forward, GCAGCAACGGGACCATTCT; reverse, CCCCATGACTAAGTCCTTCAACT);
Acaca (forward, ATGGGCGGAATGGTCTCTTTC; reverse, TGGGGACCTTGTCTTCATCAT);
Fasn (forward, GGAGGTGGTGATAGCCGGTAT; reverse, TGGGTAATCCATAGAGCCCAG);
Hmgcs (forward, AACTGGTGCAGAAATCTCTAGC; reverse, GGTTGAATAGCTCAGAACTAGCC); Hmgcr (forward, AGCTTGCCCGAATTGTATGTG; reverse, TCTGTTGTGAACCATGTGACTTC);
Sqle (forward, ATAAGAAATGCGGGGATGTCAC; reverse, ATATCCGAGAAGGCAGCGAAC);
Ldlr (forward, TGACTCAGACGAACAAGGCTG, reverse, ATCTAGGCAATCTCGGTCTCC);
Idol (forward, TGCAGGCGTCTAGGGATCAT; reverse, GTTTAAGGCGGTAAGGTGCCA);
Abca1 (forward, AAAACCGCAGACATCCTTCAG; reverse, CATACCGAAACTCGTTCACCC);
Abcg1 (forward, CTTTCCTACTCTGTACCCGAGG; reverse, CGGGGCATTCCATTGATAAGG);

Ifng (forward, ATGAACGCTACACACTGCATC; reverse, CCATCCTTTTGCCAGTTCCTC).

2.8. Measurement of the cholesterol level

Cell cholesterol levels were quantified using the Amplex Ultra Red cholesterol assay kit (Invitrogen). Briefly, 1×10^6 tumor cells or CD8+ TILs isolated by flow sorting from LKR13 tumors were homogenized in 200 µL chloroform-methanol (v/v 2:1), and the homogenates were centrifuged for 5–10 min at 14,000 rpm in a microcentrifuge. The organic phase was then transferred to a clean tube and vacuum dried. The dried lipids/cholesterol were re-dissolved in 1X concentration of component E reaction buffer. Cholesterol ester was calculated by subtracting free cholesterol levels (esterase added) from total cholesterol (no esterase).

2.9. Statistical analysis

All in vitro assays were performed at least in triplicate. Five to nine mice per group were used for the in vivo studies. General statistical analyses were performed using GraphPad Prism 7.0. An unpaired, two-tailed Student's *t*-test, or one-way ANOVA were used for column, multiple column, and group analyses, respectively. $^{*}P< 0.05$, $^{**}P< 0.01$, and $^{***}P< 0.001$ were considered statistically significant.

3. Results

3.1. Avasimibe shifts the balance from regulatory to effector T cells and increases CD8+ T cell infiltration in lung tumors

CD8+ *T* cell infiltration is a critical component of immune-mediated anti-cancer efficacy. Using the LKR13 syngeneic tumor model, we found that avasimibe treatment leads to accumulation of CD8+ *T* cells in Kras mutant lung tumor tissues (Fig. 1a and 1c). CD3+CD8+ *T* cells were observed to increase from ~20% in untreated controls to ~40% in tumor tissue of mice treated with avasimibe for one week. To differentiate whether the higher CD8+ *T* cell infiltration is caused by increased lymphocyte proliferation as opposed to CD8+ *T* cell migration, we examined Ki-67 levels of tumor-infiltrating T cells by flow cytometry and found no relevant differences in intratumoral CD8+ *T* cell proliferation (data not shown), suggesting that increases in CD8+ *T* cell presence resulted from changes in intratumoral migration. We next checked whether avasimibe changed the ratio of regulatory T cells and effector T cells in the tumor microenvironment (TME), another factor known to be critical for effective anti-tumor immune responses. Analysis of CD4+CD25+Foxp3+ Tregs in LKR13 tumors after avasimibe treatment showed time-dependent decrease in Tregs from ~50% to ~30% (Fig. 1b and c). Additionally, we observed that avasimibe treatment reduced the percentage of monocytic cells with an immunosuppressive MDSC phenotype (CD11b+Ly6C+Ly6G-) within tumors (Fig. 1d).

Additional changes in intratumoral T cell subsets were also noticeable with avasimibe treatment. For example, the population of effector memory CD4+ and CD8+ *T* cells were increased, whereas the population of central memory cells and naïve T cells were decreased (Fig. 1e and f). Moreover, we found that avasimibe treatment enhanced the tumor-infiltrating CD8+ *T* cells that expressed effector proteins such as granzyme B, IFN-γ and TNF-α (Fig. 1g).

3.2. Avasimibe treatment improves the anti-tumor efficacy of a Kras-specific multipeptide vaccine

We next investigated whether the avasimibe-induced CD8+ *T* cell tumor infiltrates could generate anti-tumor immune responses in a $Kras^{G12D}$-driven lung tumor syngeneic model when combined with KVax. To test this, we vaccinated 6-week old mice with Kras peptides and CpG/R858/FGK adjuvant, followed by three boost vaccinations administered at two-week intervals (Fig. 2a). LKR13 tumor cells were injected subcutaneously into the flanks of wild-type sv129 mice one week after the final boost vaccine, and tumor growth was monitored in the presence or absence of avasimibe administration. We found that treatment with either avasimibe or KVax alone significantly decreased tumor burden, and the combination of the KVax and avasimibe worked additively to inhibit tumor growth (70% decrease relative to adjuvant-treated controls) (Fig. 2b).

To test whether functional immune responses induced by KVax were enhanced by avasimibe, we performed IFN-γ based ELISPOT assays of splenocytes isolated from adjuvant-treated controls or Kras-vaccinated mice. T cells from vaccinated animals demonstrated a robust antigen-specific IFN-γ response when re-stimulated with KVax peptides (Fig. 2c, upper left panel). Additionally, we tested whether vaccine-induced T cells could also recognize endogenously processed $Kras^{G12D}$ in tumor cells by testing splenocytes isolated from vaccinated animals with LKR13 tumor cells for production of IFN-γ, granzyme B, and TNF-α secretion in ELISPOT assays. As shown in Fig. 2c, when pulsed with LKR13 tumor cells, splenocytes from the vaccinated mice showed significantly increased frequencies of IFN-γ-secreting T cells (Fig. 2c, upper right panel) and a trend toward increased frequencies of T cells secreting granzyme B or TNF-α, (Fig. 2c lower panel). These results indicate that T cell responses elicited by KVax are specific to Kras peptides, and help facilitate an endogenous anti-tumor response. There was no evidence of nonspecific immune activation as none of the animals responded to an irrelevant antigen (HIV peptides), further supporting the notion that the immune response detected in the vaccinated group was highly specific to the KVax.

3.3. Combined treatment with avasimibe and KVax increases T cell immunity

To further define the basis of increased antitumor efficacy observed after combined treatment with avasimibe and KVax, we evaluated cell surface phenotype and intracellular cytokine production in T cells isolated from tumors and spleens collected at the end of the efficacy study shown in Fig. 2. The analyses confirmed that avasimibe treatment alone increased the frequencies of tumor-infiltrating CD8+ *T* cells whereas the frequency of CD4+ *T* cells remained unchanged (Fig. 3a). KVax treatment alone significantly increased both intratumoral CD8+ and CD4+ *T* cell frequencies (Fig. 3b). The combination of avasimibe plus KVax further increased the frequencies of tumor infiltrating CD8+ *T* cells, but not tumor infiltrating CD4+ *T* cells (Fig. 3b). We then evaluated the activity of these T cells by assessing IFN-γ production-(Fig. 3c). The percentages of CD8+ *T* cells secreting IFN-γ were significantly increased after Kras vaccination and remained high in the combination group, while granzyme B and TNF-α levels were not significantly changed (data not shown). When re-stimulated with non-antigen stimuli PMA/Ionomycin, T cells from mice treated with avasimibe or KVax treatment generated increased IFN-γ, granzyme B and TNF-α secretion in CD8+ TILs, and T cells obtained from mice after combination treatment demonstrated the greatest increase (Fig. 3d and e).

3.4. Avasimibe modulates cholesterol metabolism primarily in CD8+ T cells

To determine the biochemical basis for the increased effector function and enhanced tumor-infiltrating CD8+ *T* cell frequencies

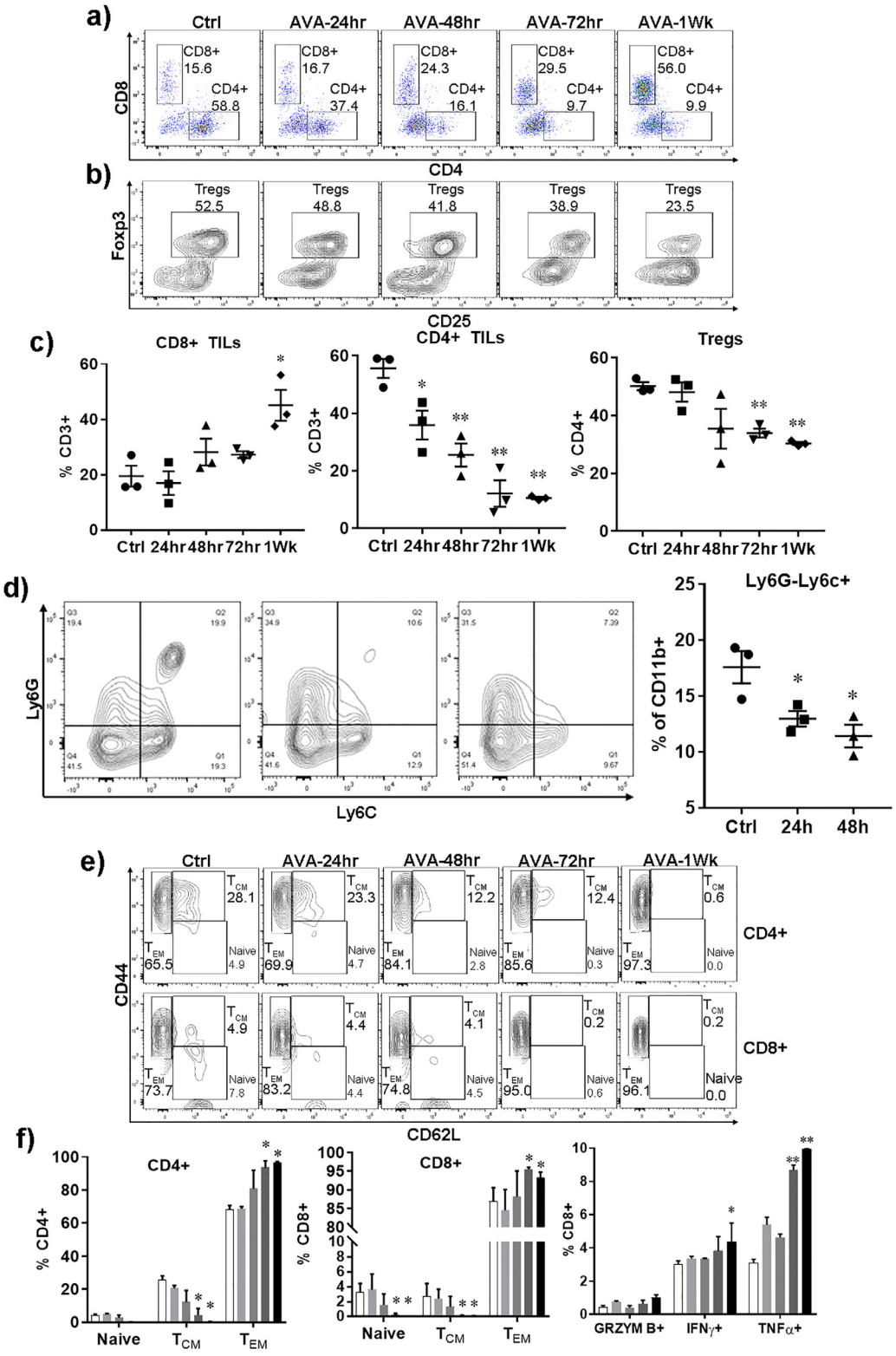

Fig. 1. Avasimibe shifts the balance from regulatory to effector T cells and increases CD8+ *T* cell infiltration in lung tumors. Kras-driven LKR13 mouse lung cancer cells were inoculated into sv129 mice, i.p. treatments with avasimibe (AVA) were started at different time points when tumors reached ~200mm[3] in size. At the experimental endpoint, tumors were processed into single cell suspension, enriched for TILs by Ficoll gradient separation, and flow cytometric analysis was conducted on the tumor-infiltrating leukocytes isolated from control or AVA-treated LKR13 lung tumors. (a, b) Representative flow cytometric histograms for CD4 and CD8 T cells and Tregs in the TME. (c) Percentages of CD8+, CD4+ and Tregs in the TME. (d) Representative flow cytometric histograms and results for monocytic cells n TME. (e) Representative flow cytometric histograms and combined results for staining of cells with CD44 and CD62L to assess naïve T cells, T_{CM} and T_{EM} cells. (f-g) Flow cytometric histograms and combined results for staining of cells for intracellular cytokines granzyme B, IFN-γ and TNF-α after stimulation with PMA and Ionomycin. Data are shown as the mean ± SE of three replicate samples per group, $n = 3$, $^{*}P \leq 0.05$ vs Ctrl, two-tailed Student's *t*-test.

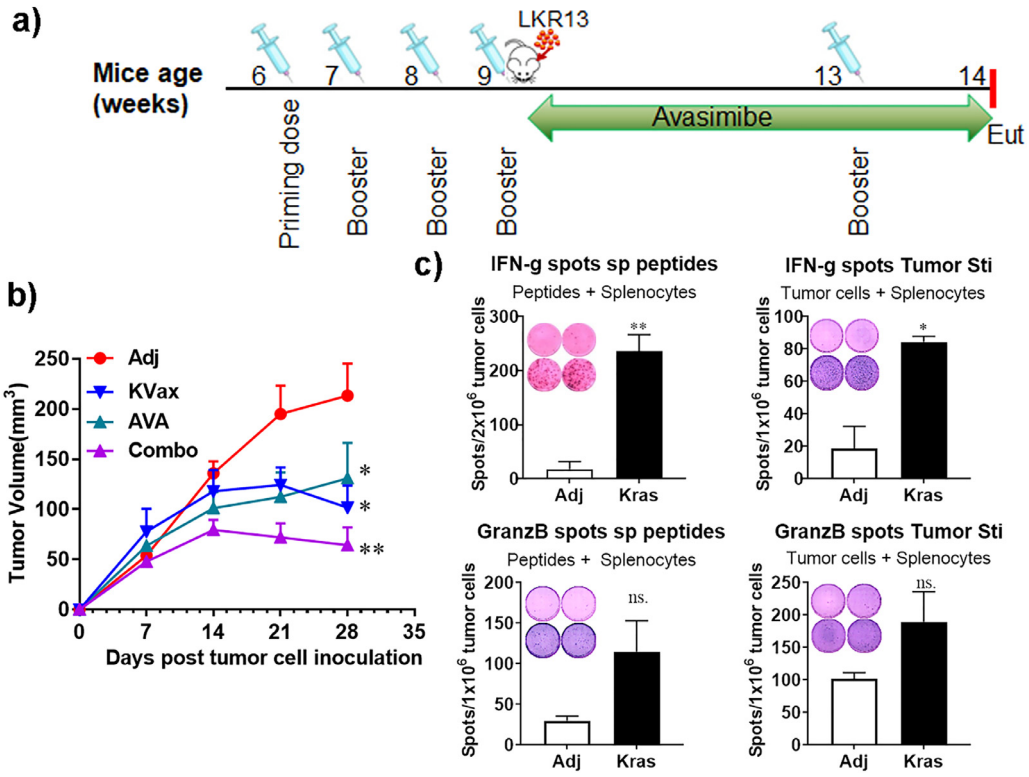

Fig. 2. AVA plus the Kras peptide vaccine enhances the inhibition of lung tumor progression in a syngraft model. (a) Experimental design outlining the timing of vaccine and AVA administration, inoculation of tumor cells, and the experimental endpoint (Eut, euthanasia). Sv129 mice were given 4 weekly Kras multipeptide vaccinations, the Kras-driven mouse lung cancer cell LKR13 was then injected, and avasimibe treatments were given every other day until the experimental endpoint. Tumor sizes were measured weekly. The experiment was repeated three more times. (b) Tumor volume quantitation over time. (c) Representative ELISPOT assay figures (insets) and combined results. Upper left panel, splenocytes controls or Kras-vaccinated animals re-stimulated with a combination of KRAS peptides (p5–21, p5–21 G12D, p17–31, and p78–92). Upper right and lower panels, splenocytes re-stimulated with LKR13 cancer cells. Combined results are the mean ± SE, $n = 10$, $^{*}P \leq 0.05$, $^{**}P \leq 0.01$, $^{***}P \leq 0.001$ vs Ctrl, two-tailed Student's *t*-test.

resulting from avasimibe treatment, we measured the free cholesterol (FC) level in tumor tissues from animals treated with vehicle or avasimibe. Whereas we found no significant change in FC in tumor cells (Fig. 4a, left panel), we found that cholesterol ester levels were decreased significantly in avasimibe-treated CD8+ TILs (Fig. 4a, right panel), confirming that avasimibe inhibits the conversion of free cholesterol to cholesteryl ester in CD8+ *T* cells. To determine how free cholesterol level were raised in avasimibe treated CD8+ TILs, we measured the transcriptional levels of cholesterol metabolism genes. After flow-sorting either tumor cells or CD8+ TILs from LKR13 tumors (Sup Fig. 1) and treating them with a range of doses of avasimibe, we examined the key genes involved in cholesterol metabolism, including those involved in biosynthesis and transport of cholesterol in cancer cells and CD8+ TILs. We found that CD8+ *T* cells expressed higher mRNA levels of cholesterol metabolism pathway genes as compared to cancer cells (Fig. 4b); including ACACA, Srebp, and Hmgcr, which are involved in cholesterol synthesis, and Abcg and Abca genes, which are involved in cholesterol transport. In contrast, treatment of cancer cells with avasimibe resulted only in changes in Abcg1 (Fig. 4c lower two panels), whereas mRNA levels of the other genes were not affected. Treatment of CD8+ TILs with avasimibe also induced dose-dependent increases in several genes essential for cholesterol synthesis (e.g., Fasn, Hmgcr, Hmgcs, and Idol (Fig 4c, upper left panel), as well as modest up-regulation in the levels of cholesterol transport and cholesterol ester hydrolysis genes (Fig. 4c upper right panel). These results indicate that avasimibe not only causes less conversion of free cholesterol to cholesteryl esters by inhibiting ACAT1 as demonstrated in earlier studies, but it also promotes more cholesterol biosynthesis, thereby increasing cholesterol levels, which in turn may enhance TCR clustering, signaling and the eventual potentiation of T cell effector function.

3.5. Increased T cell infiltration by avasimibe improves KVax anti-tumor efficacy in the Kras^{la1} lung cancer model

Previously, we demonstrated that a multi-peptide KVax can prevent lung tumorigenesis prior to the onset of Kras mutations. However, it is likely that efficacy in this circumstance would be of little translational value since humans at high-risk of developing lung cancer would likely already have dysplastic cells expressing mutant Kras. Therefore, to test the multi-peptide KVax in a murine model that more closely recapitulates the molecular profile of high-risk patients, we used the Kras^{LA1} murine model which initiates expression of mutant Kras^{G12D} at an endogenous locus immediately after birth. Since Kras is expressed at high levels in the lungs shortly after birth, this model has proven to more closely model clinical lung tumorigenesis and ideal for prevention studies, where Kras is targeted in the presence of pre-existing mutations.

Beginning at 5 weeks of age, we treated Kras^{LA1} mice with four bi-weekly vaccinations, followed by monthly boost vaccines until the end of the study; oral avasimibe treatment was initiated after completion of the fourth vaccination until the end of the study (Fig. 5a). KVax alone or avasimibe alone was able to inhibit Kras-driven lung tumorigenesis in the Kras^{LA1} model (Fig. 5b), and the combination therapy trended toward improved anti-cancer efficacy when compared with individual treatment (Fig. 5b, right panel). While mice treated with KVax plus avasimibe had similar numbers of tumors as compared to the KVax alone or avasimibe alone, the tumors were smaller in the mice treated with both KVax and

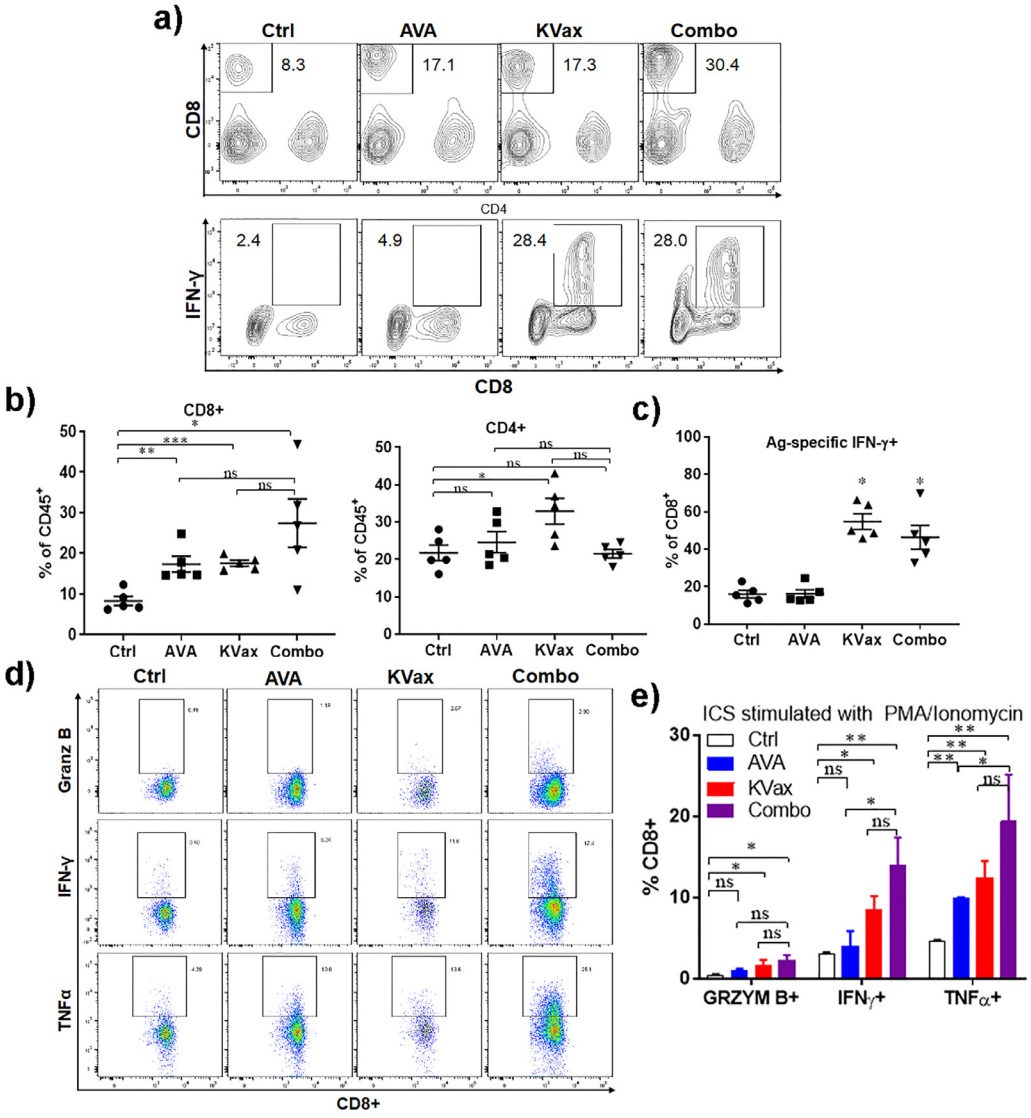

Fig. 3. Immunophenotyping of T cells from syngraft tumors of animals treated with AVA and/or KVax. Tumors and spleens were collected at the efficacy study experimental endpoint from LKR13 bearing mice as shown in Fig. 2. (a) Representative flow cytometry graphs showing CD8+ and IFN-γ staining cells. (b, c) Combined treatment with AVA and KVax promotes increased frequencies of tumor-infiltrating CD8+ *T* cells. (d, e) Combined treatment with AVA and KVax leads to increased cytokine-producing CD8+ *T* cells. Data are shown as the mean ± SE of three replicate samples per group, $n = 5$, $^{*}P \leq 0.05$, $^{**}P \leq 0.01$, $^{***}P \leq 0.001$ vs Ctrl, one-way ANOVA.

avasimibe; further, the tumors in the mice that received the combined treatment were mostly adenomas indicating that the combined treatment regimen also delayed tumorigenic progression to malignant disease (Sup Fig. 2). Lung tumors from animals were also evaluated using IHC staining for the expression level of proliferative markers (Ki-67) and apoptotic markers (Caspase-3). Our results show that while treatment with KVax or avasimibe decreased the proliferation, the combination led to substantially greater decrease for cell proliferation (Fig. 5c). In our study, we didn't find a significant change in apoptosis for all treated groups (data not shown).

To verify if avasimibe, KVax, or the combination also increased CD8+ *T* cell infiltration in $Kras^{LA1}$ tumors, we performed IHC staining and compared the percentage of CD8+ *T* cells present in lung tumors. While avasimibe or KVax alone each increased CD8+ *T* cells in tumors (Fig. 5d), the combination treatment increased CD8+ *T* cell infiltration to the greatest extent.

Cytokine/chemokine analysis was also conducted using splenocytes isolated from $Kras^{LA1}$ mice treated with adjuvant control, KVax, avasimibe or combination of avasimibe and KVax (Fig. 5e). We observed robust increases in IFN-γ such that it increased after treatment greater than all other 32 cytokine/chemokines tested, both individually after avasimibe and KVax, and to a greater extent with combination treatment. Other than IFN-γ, G-CSF, IL-6, KC, MIG, LIX, TNFα were also increased after treatments.

4. Discussion

Previously, we demonstrated that multiple long Kras-specific peptides [15–20 amino acids (AA)] against both wild-type and G12D mutant forms of Kras can effectively prevent development of mutated lung cancer in mice. These peptides are conserved between humans and mice, and are predicted to have high-affinity binding to multiple MHC class II alleles for both species [4]. Vaccination with these peptides in the primary prevention setting (vaccination before Kras activation) in the CCSP-Kras lung cancer model has shown striking efficacy, resulting in >80% decrease in tumor volume [4]. However, in high risk patients, Kras mutations exist long before tumor onset, and constitutively active Kras expression could induce an immune suppressive environment dur-

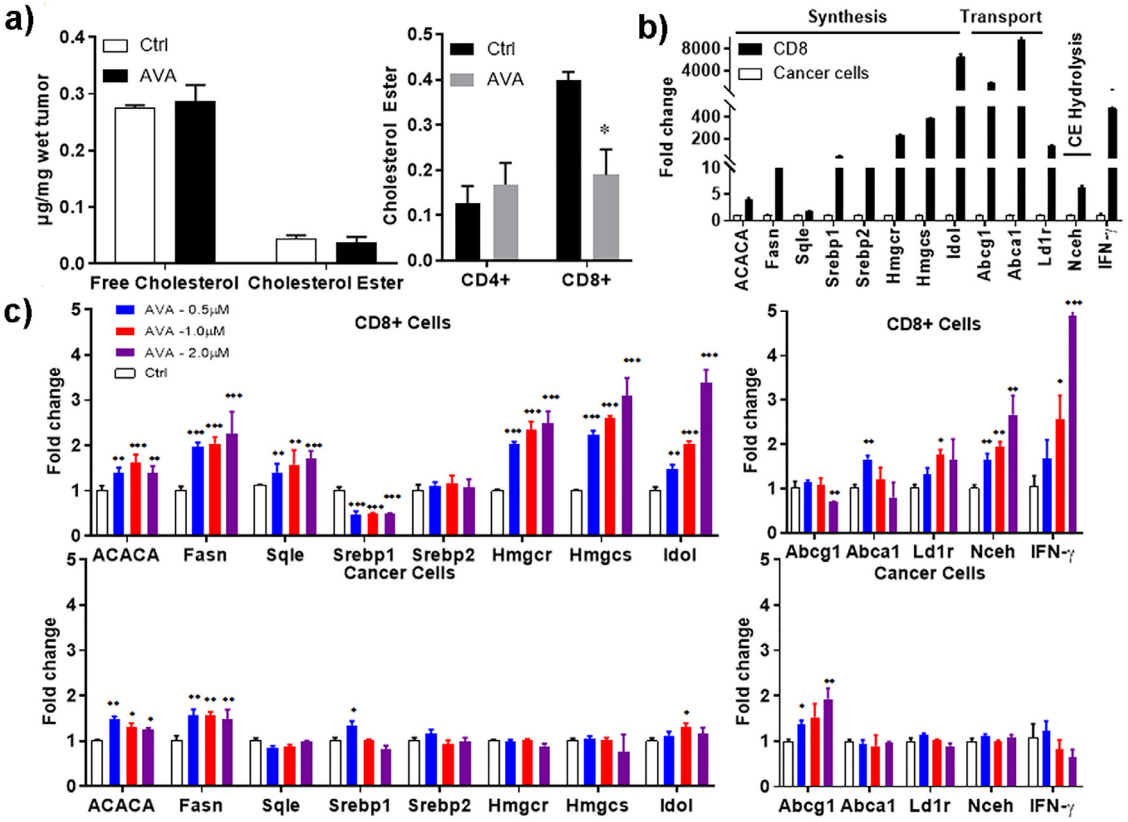

Fig. 4. AVA modulates the cholesterol levels in CD8+ *T* cells. (a) Free cholesterol and cholesterol ester levels were measured in tumor cells and T cells isolated from LKR13 tumors using Amplex Ultra Red. (b) Comparison of cholesterol esterification gene transcription levels in CD8+ TILs as compared to cancer cells. (c) Upregulation of cholesterol synthesis and cholesterol transport gene transcription levels by AVA in cancer cells and CD8+ TILs when compared to non-treated controls. Data are shown as the mean ± SE of three replicate samples per group, $n = 3$, $^{*}P \leq 0.05$, $^{**}P \leq 0.01$, $^{***}P \leq 0.001$ vs Ctrl, one-way ANOVA.

ing lung tumorigenesis [19], which might hamper preventive efficacy of the KVax. We therefore hypothesized that an innovative combinatorial chemoimmunopreventive approach consisting of MHC class II-restricted Th1-promoting Kras peptide vaccines plus avasimibe, each with unique and complementary mechanisms of action, will provide optimal efficacy to prevent Kras-driven lung carcinogenesis and progression in clinically relevant Kras mutant lung cancer models. In the current study, we show that this combinatorial approach elicited improved anti-tumor efficacy in both a syngraft model as well as a GEMM model, where Kras activation was initiated long before vaccination.

Previous research has established a strong link between cholesterol esterification and cancer development and progression [20–23]. Aberrant accumulation of cholesteryl ester is mediated by ACAT1 [24]. Avasimibe, a potent inhibitor of ACAT-1, has been shown to suppress the proliferation of various human cancer cell lines in vitro including lung, prostate, pancreas, colon, and chronic myelogenous leukemia, and the growth of various tumor xenografts in vivo [20–23]. However, a recent study showed that cholesterol metabolism regulates the function of anti-tumor $CD8^{+}$ cytotoxic T cells [13]. Based on results from earlier studies, we postulated that avasimibe treatment could have beneficial anti-tumor effects in lung cancer. While 20 μM avasimibe has been reported to decrease cholesterol esterification in several tumor cells or tissues, the steady state in vivo concentration of avasimibe is only about 1 μM [21]. We measured the cholesterol levels in tumor cells and $CD8^{+}$ TILs and found that doses of avasimibe used in vivo modulate cholesterol metabolism primarily in CD8+ *T* cells. ACAT1 blockade with avasimibe led to higher mRNA levels of cholesterol biosynthesis genes in CD8+ TILs when compared with cancer cells, whereas the levels of cholesterol transport and cholesterol ester hydrolysis genes underwent modest changes (Fig. 4). These results indicate that ACAT1 blockade not only caused less conversion of free cholesterol to cholesteryl esters (Fig. 4a right panel), but might also cause more cholesterol biosynthesis, which could result in the higher plasma membrane cholesterol level on CD8+ *T* cells. Previous studies already demonstrated that plasma membrane cholesterol levels correlate with the effector function of CD8+ *T* cells, and addition of plasma membrane cholesterol led to potentiated effector function. Therefore, the effect of avasimibe on cholesterol metabolism may contribute to the increased CD8+ *T* cell function that we observed in Fig. 1, and ultimately the inhibition of tumor progression. Fatty acid metabolism has also been linked with a proliferative advantage for regulatory T cells [25]. In our current study, we found that avasimibe reduced numbers of CD4+CD25+Foxp3+ regulatory T cells in the TME, while promoting effector T cell expansion and function. The decrease in CD4+ Tregs, as well as the increase in CD8+ *T* cells, are most likely responsible for the decrease in relative percentages of CD4+ *T* cells within the CD3 compartment.

Th1 immunity is critical for immunotherapy-mediated cancer eradication. MHC II-restricted peptide vaccines elicit tumor antigen-specific Th1 immunity and orchestrate tumor-reactive $CD8^{+}$ CTL responses by increasing the amount of antigen available to $CD8^{+}$ *T* cells. We identified Kras-specific epitopes by using the "combined scoring system" to identify peptides that bind with optimal affinity and induce high levels of the cytokine IFN-γ, but not Th1 immune inhibitory cytokines such as IL-10 [4]. This approach allowed us to identify vaccine candidate peptides that induce optimal type I immune response instead of detrimental Th2 responses

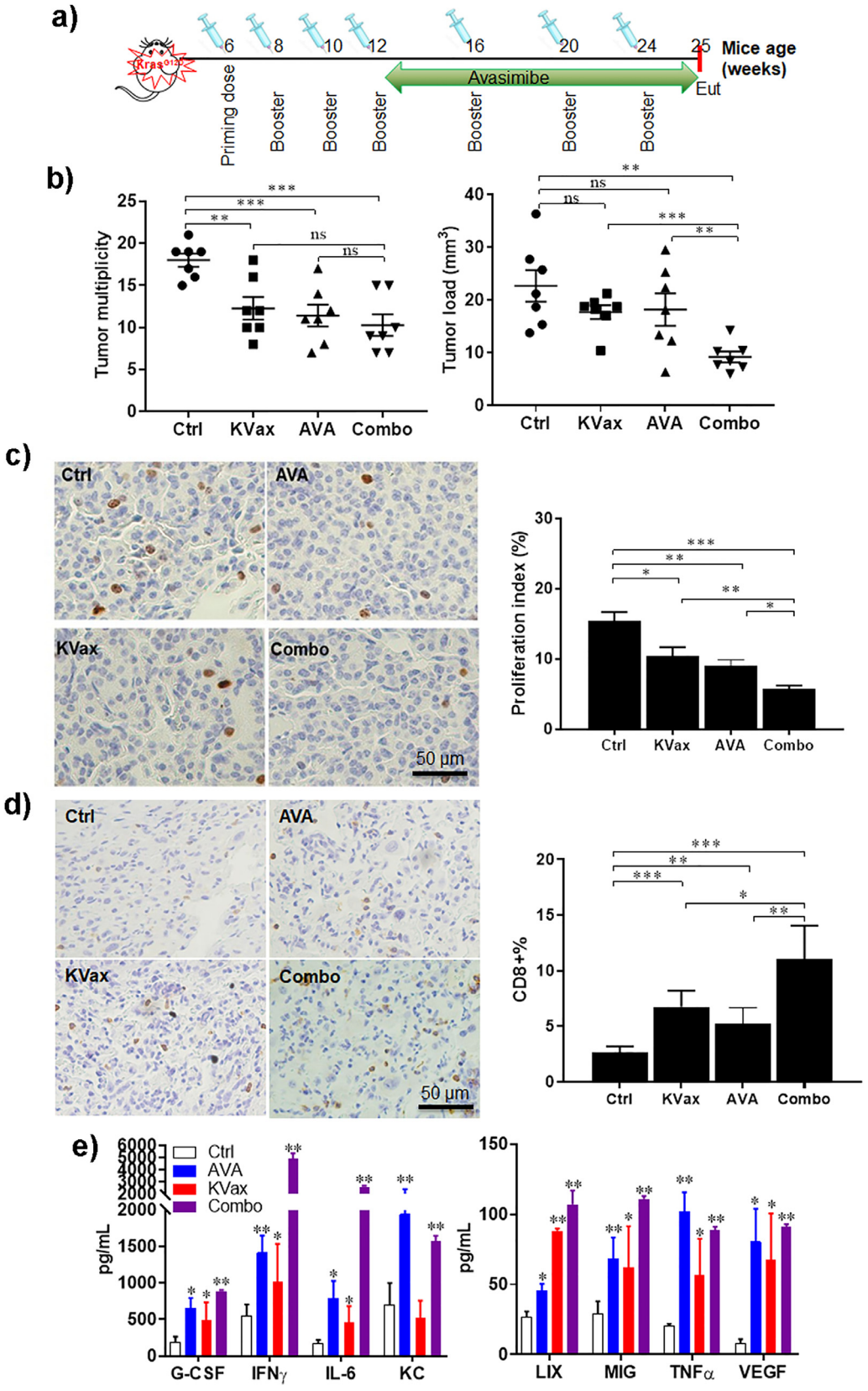

Fig. 5. The combination of AVA with KVax enhances the inhibition of Kras-driven lung tumors in the Kras^{LA1} GEMM model. (a) Experimental design outlining the timing of vaccine, AVA administration, and experimental endpoint (Eut, euthanasia). (b) Tumor multiplicity and tumor volume quantitation at the experimental endpoint. (c) Representative IHC staining and quantitative data for Ki-67 from the Kras^{LA1} model lung tumor. (d) Representative IHC staining and quantitative data for tumor-infiltrating CD8+ *T* cells from the Kras^{LA1} model lung tumor. (e) Cytokine analysis by Mouse Cytokine Array/ Chemokine Array 31-Plex (MD31) using supernatant collected from splenocytes stimulated with peptides for 72hr. Data are shown as the mean ± SE, $n = 8$, $^{*}P \leq 0.05$, $^{**}P \leq 0.01$, $^{***}P \leq 0.001$ vs Ctrl, two-tailed Student's *t*-test.

[4]. Using this approach, we developed a MHC class II-restricted Kras multi-peptide vaccine that targets wild-type Kras regions, and we showed that the $Kras^{wt}$ vaccine induces potent Th1 helper responses that led to greater than 80% inhibition of Kras-driven lung tumorigenesis, with no overt toxicity to normal tissues and organs [4]. Our results showed that the combination of KVax (targeting $CD4^+$) and avasimibe (driving $CD8^+$ CTL) induced a better type I adaptive immune response and tumor protection than monotherapy with either treatment alone. The expression of CTL effector cytokines (IFN-γ, TNF-α) and cytotoxic effector molecules (granzyme B) were all upregulated in animals given the combined treatment.

In summary, we have shown that our Kras-peptide-based vaccine, which targets not only mutant $Kras^{G12D}$ but other wild-type regions, can be combined with avasimibe to improve inhibition of Kras-driven lung tumorigenesis. Owing to the promiscuous binding of these Kras peptides to both human and mouse MHC II alleles, our studies in mouse lung cancer models bear strong clinical relevance and translational potential. These mutant epitopes are 100% identical to human mutant KRAS, and are thus of high translational potential, particularly for preventing tumorigenesis in patients with precancerous lesions. These results established a "proof-of-principle" that can be directly translated to patients with Kras-mutant lung premalignant lesions for preventing their progression to malignant lesions, and used for preventing metastasis in patients with KRAS-mutant early primary lung cancers.

5. Author contributions

M.Y., J.P. Q.Z., S.S., R.H.S., and R.A.L. were responsible for the overall experimental design with input by K.P., Q. Z. and B.J. The project was supervised by M.Y., J.P., Q.Z., B.J., Y.W., S.S., R.H.S., and R.A.L. K.P., L. Q., and J.P. conducted flow cytometry analysis, J.P. and Q.Z. assessed anti-cancer efficacy in animal models. J.P. assessed cholesterol levels and qPCR analysis of the expression level of the key cholesterol metabolism enzymes. The following were responsible for writing, reviewing, and editing the manuscript: J.P., Q.Z., B.J., S.S., R.H.S., R.A.L., L.W., Y.W., and M.Y.

Declaration of Interests

The authors declare that there are no financial or other conflicts of interest.

Acknowledgments

We are grateful to Dr. Jonathan M. Kurie (MD Anderson) for providing both $Kras^{LA1}$ mice and the LKR13 cells.

Funding Sources

This work was funded from National Cancer Institute (HHSN26100002), Drs. Shizuko Sei, Robert H. Shoemaker, and Ronald A. Lubet from NCI have participated in the study design and editing of the manuscript. This work was also supported by the grants from National Institutes of Health [R01CA223804 (M.Y.; L.W.); R01CA232433 (M.Y.); R01CA223804 (M.Y.); R01 CA164225 (L.W.)].

Supplementary materials

Supplementary material associated with this article can be found, in the online version, at doi:10.1016/j.ebiom.2019.10.044.

References

[1] Shames DS, Wistuba II. The evolving genomic classification of lung cancer. J Pathol 2014;232(2):121–33.
[2] Prior IA, Lewis PD, Mattos C. A comprehensive survey of ras mutations in cancer. Cancer Res 2012;72(10):2457–67.
[3] Cox AD, Fesik SW, Kimmelman AC, Luo J, Der CJ. Drugging the undruggable RAS: mission possible? Nat Rev Drug Discov 2014;13(11):828–51.
[4] Pan J, Zhang Q, Sei S, et al. Immunoprevention of KRAS-driven lung adenocarcinoma by a multipeptide vaccine. Oncotarget 2017;8(47):82689–99.
[5] Wojtowicz ME, Dunn BK, Umar A. Immunologic approaches to cancer prevention-current status, challenges, and future perspectives. Semin Oncol 2016;43(1):161–72.
[6] Tsai HJ. Clinical cancer chemoprevention: from the hepatitis b virus (HBV) vaccine to the human papillomavirus (HPV) vaccine. Taiwan J Obstet Gynecol 2015;54(2):112–15.
[7] Meyer RG, Korn S, Micke P, et al. An open-label, prospective phase i/ii study evaluating the immunogenicity and safety of a ras peptide vaccine plus gm-csf in patients with non-small cell lung cancer. Lung Cancer 2007;58(1):88–94.
[8] Poloso NJ, Roche PA. Association of mhc class II-peptide complexes with plasma membrane lipid microdomains. Curr Opin Immunol 2004;16(1):103–7.
[9] Gombos I, Detre C, Vamosi G, Matko J. Rafting mhc-ii domains in the apc (presynaptic) plasma membrane and the thresholds for T-cell activation and immunological synapse formation. Immunol Lett 2004;92(1–2):117–24.
[10] Janes PW, Ley SC, Magee AI, Kabouridis PS. The role of lipid rafts in t cell antigen receptor (TCR) signalling. Semin Immunol 2000;12(1):23–34.
[11] Kabouridis PS. Lipid rafts in t cell receptor signalling. Mol Membr Biol 2006;23(1):49–57.
[12] Zhao L, Li J, Liu Y, et al. Cholesterol esterification enzyme inhibition enhances antitumor effects of human chimeric antigen receptors modified t cells. J Immunother 2018;41(2):45–52.
[13] Yang W, Bai Y, Xiong Y, et al. Potentiating the antitumour response of CD8(+) t cells by modulating cholesterol metabolism. Nature 2016;531(7596):651–5.
[14] Huttunen HJ, Kovacs DM. ACAT as a drug target for alzheimer's disease. Neurodegener Dis 2008;5(3–4):212–14.
[15] Pal P, Gandhi H, Giridhar R, Yadav MR. ACAT inhibitors: the search for novel cholesterol lowering agents. Mini Rev Med Chem 2013;13(8):1195–219.
[16] Zhong L, Roybal J, Chaerkady R, et al. Identification of secreted proteins that mediate cell-cell interactions in an in vitro model of the lung cancer microenvironment. Cancer Res 2008;68(17):7237–45.
[17] Johnson L, Mercer K, Greenbaum D, et al. Somatic activation of the K-ras oncogene causes early onset lung cancer in mice. Nature 2001;410(6832):1111–16.
[18] Zhang Q, Pan J, Lubet RA, et al. Enhanced antitumor activity of 3-bromopyruvate in combination with rapamycin in vivo and in vitro. Cancer Prev Res (Phila) 2015;8(4):318–26.
[19] Nasti TH, Rudemiller KJ, Cochran JB, et al. Immunoprevention of chemical carcinogenesis through early recognition of oncogene mutations. J Immunol 2015;194(6):2683–95.
[20] Li J, Gu D, Lee SS, et al. Abrogating cholesterol esterification suppresses growth and metastasis of pancreatic cancer. Oncogene 2016;35(50):6378–88.
[21] Lee SS, Li J, Tai JN, Ratliff TL, Park K, Cheng JX. Avasimibe encapsulated in human serum albumin blocks cholesterol esterification for selective cancer treatment. ACS Nano 2015;9(3):2420–32.
[22] Bandyopadhyay S, Li J, Traer E, et al. Cholesterol esterification inhibition and imatinib treatment synergistically inhibit growth of bcr-abl mutation-independent resistant chronic myelogenous leukemia. PLoS ONE 2017;12(7) e0179558.
[23] Yue S, Li J, Lee SY, et al. Cholesteryl ester accumulation induced by pten loss and PI3K/AKT activation underlies human prostate cancer aggressiveness. Cell Metab 2014;19(3):393–406.
[24] Silvente-Poirot S, Poirot M. Cholesterol and cancer, in the balance. Science 2014;343(6178):1445–6.
[25] Lochner M, Berod L, Sparwasser T. Fatty acid metabolism in the regulation of t cell function. Trends Immunol 2015;36(2):81–91.